Optical isolation based on nonreciprocal phase shift induced by interband photonic transitions

Zongfu Yu[a] and Shanhui Fan
Ginzton Lab, Stanford University, Stanford, California 94305, USA

(Received 5 February 2009; accepted 12 April 2009; published online 1 May 2009)

Photonic transitions in waveguides can create nonreciprocal phase response for counterpropagating modes. Such effect can be used in Mach–Zehnder interferometers to form optical isolators and circulators. Performance of such device is analyzed using coupled mode theory given the experimentally available modulation in silicon. The proposed scheme can provide a broadband (>0.8 THz), high contrast ratio (>20 dB) optical isolation at telecommunication wavelength. © *2009 American Institute of Physics*. [DOI: 10.1063/1.3127531]

The lack of physical mechanism for on-chip signal isolation has been a fundamental roadblock in integrated optics.[1] Magneto-optical materials, commonly used in bulk optics for signal isolation purposes, prove to be very difficult to integrate especially on a silicon photonics platform.[2–5] Thus, there has been intense interest for developing optical isolation schemes without using magneto-optical effects.[6–8] In this context, here we introduce a dynamic isolator structure, as shown in Fig. 1(a), which allows one-way light transmission while completely prohibiting the transmission of light signal in the opposite direction.

The proposed device in Fig. 1(a) is based upon the recent discovery of complete optical isolation effect induced by dynamic modulation.[8] The isolation scheme in Ref. 8 used a silicon waveguide that supports two modes with opposite symmetries forming two photonic bands [Fig. 1(b)]. When subject to a refractive index modulation that is both spatial and temporal dependent, as defined by a modulation frequency and a wave vector, the modes inside the waveguide can go through an interband transition[9] [Fig. 1(c)]. Such a transition is highly nonreciprocal: the modulation breaks both time-reversal and spatial inversion symmetry. As a result, interband photonic transition process occurs only along the forward direction but not in the backward direction. By choosing an appropriate length of the modulation region, complete frequency conversion can be achieved in the forward direction, while no conversion occurs in the backward direction. (This length is referred to as the coherence length l_c below). In this construction, complete isolation is accomplished by combining the nonreciprocal frequency conversion process, as discussed above, with a filter that removes all the converted light.[8]

In this letter, we present an alternative geometry for constructing an optical isolator. The geometry consists of a Mach–Zehnder interferometer, in which one arm of the interferometer consists of the waveguide that is subject to the dynamic modulation described above. In contrast to Ref. 8, here the length of the modulation region is chosen to be twice the coherence length. Thus, light passing through the modulated waveguide will remain in the incident frequency. As we will show below, however, such light in fact experiences a phase shift that is nonreciprocal due to the photonic transition effect. The use of a Mach–Zehnder interferometer configuration thus allows an optical isolator to be formed [Fig. 1(a)]. Comparing with the scheme in Ref. 8 here the filter is no longer required, which significantly reduces the device complexity.

We describe the Mach–Zehnder isolator by first briefly reviewing the interband transition process in a silicon slab waveguide. The width d of the waveguide [Fig. 1(b)] is chosen such that the waveguide supports two TE (transverse electric) bands, with even or odd symmetry, respectively, at the operation frequency. An interband transition, between two TE modes with frequencies and wave vectors (ω_1,k_1) and (ω_2,k_2) located in the two bands, respectively [Fig. 1(c)], can be induced by a dielectric constant modulation: $\varepsilon'(x,z,t)=\delta(x)\cos(\Omega t+qz)$, where $\delta(x)$ describes the modulation profile in the transverse direction, and the modulation frequency $\Omega=\omega_2-\omega_1$. (In what follows, the subscripts in k

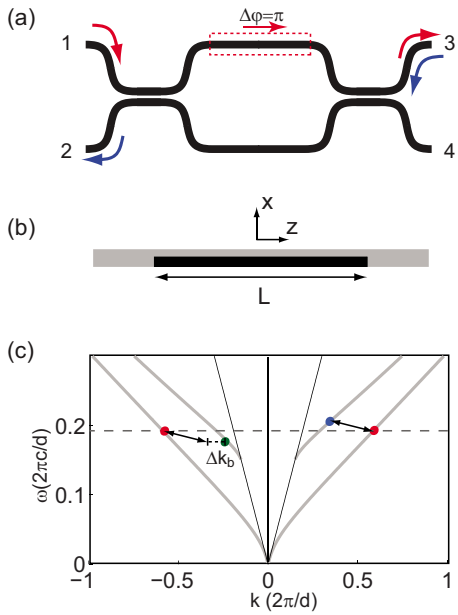

FIG. 1. (Color online) (a) Schematic of an optical isolator based on Mach–Zehnder interferometer. The dynamic index modulation is applied to the waveguide in the dashed red box. The structure of the modulated silicon waveguide is shown in (b), where the dynamic index modulation is applied to the black region. (c) The dispersion relation of the TE modes. The phase-matching modulation (arrow) induces a photonic transition between modes at ω_1 (red, dashed line) and ω_2 (blue, above the dashed line) in the forward direction. In the backward direction, the arrow represents the transition with the smallest phase mismatch.

[a]Electronic mail: zfyu@stanford.edu.

will be used to refer to the two bands.) We choose $\delta(x)$ to be nonvanishing over half of the cross section of the waveguide, so that these two modes of different spatial symmetries can couple.

In the modulated waveguide, the transition process is described by writing the total electric fields in the waveguide as $\Sigma_{i=1,2}a_i(z)E_i(x)e^{i(-k_iz+\omega_it)}$, where E_i are modal profiles normalized such that $|a_i|^2$ represent the photon number flux. Assuming incident light into the modulated waveguide having the lower frequency ω_1 [Fig. 1(b)], the amplitudes of two modes at the end of modulated region can be obtained by a spatial coupled mode theory[8]

$$a_1(z) = e^{-iL\Delta k/2}\left\{\cos\left[\frac{L}{2l_c}\sqrt{\pi^2+(l_c\Delta k)^2}\right] + i\frac{l_c\Delta k}{\sqrt{\pi^2+(l_c\Delta k)^2}}\sin\left[\frac{L}{2l_c}\sqrt{\pi^2+(l_c\Delta k)^2}\right]\right\}a_1(0) \equiv Ta_1(0),$$

$$a_2(z) = ie^{iL\Delta k/2}\frac{\pi\sin\left[\frac{L}{2l_c}\sqrt{\pi^2+(l_c\Delta k)^2}\right]}{\sqrt{\pi^2+(l_c\Delta k)^2}}a_1(0), \tag{1}$$

where $\Delta k=k_2(\omega_2)-k_1(\omega_1)+q$ is the phase mismatch, and the coherent length

$$l_c = \frac{2\pi}{\gamma}\sqrt{\frac{v_{g1}v_{g2}}{\omega_1\omega_2}} \approx \lambda_0\cdot\frac{1}{\gamma}\cdot\frac{v_g}{c}, \tag{2}$$

where $\gamma=\int_{-\infty}^{\infty}\delta(x)E_1(x)E_2(x)dx/\sqrt{\int_{-\infty}^{\infty}\varepsilon(x)|E_1|^2dx\int_{-\infty}^{\infty}\varepsilon(x)|E_2|^2dx}$ characterizes the effect of modulation, and is referred to as the modulation strength factor below. v_{gi} are the group velocities of the two modes. In arriving at the final result in Eq. (2), we have assumed that the modulation frequency is small compared with the optical frequency, hence $\omega_1\approx\omega_2$. Here, and also in the rest of the paper, we have assumed that the two bands have similar group velocity, i.e., $v_{g1}=v_{g_2}\equiv v_g$, which is essential for broadband operation.[8] λ_0 is the operating wavelength and c is the speed of light in vacuum. We note that such a coupled-mode theory result has been fully validated with full-field finite-difference time-domain simulations.[8]

We now consider the property of the Mach–Zehnder interferometer of Fig. 1(a), where the upper arm is modulated. We assume that the interferometer has two arms with equal length, and uses two 50/50 waveguide couplers. For such an interferometer, the transmission at frequency ω_1 is described by[10]

$$\begin{pmatrix} b_u \\ b_l \end{pmatrix}_{\mathrm{OUT}} = \frac{1}{2}\begin{pmatrix} 1 & i \\ i & 1 \end{pmatrix}\begin{pmatrix} T\exp(i\varphi_p) & 0 \\ 0 & \exp(i\varphi_p) \end{pmatrix}\begin{pmatrix} 1 & i \\ i & 1 \end{pmatrix} \times\begin{pmatrix} b_u \\ b_l \end{pmatrix}_{\mathrm{IN}}, \tag{3}$$

where $b_{u/l}$ is the input or output amplitudes in the upper/lower arm and φ_p is the phase due to propagation only. T, as defined in Eq. (1), is the amplitude transmission coefficient for the modulated waveguide.

To describe the isolator action, we first consider light injected into port 1. Assuming a phase-matching modulation, i.e., $\Delta k_f=k_2(\omega_2)-k_1(\omega_1)+q=0$, and a length of modulated region $L=2l_c$, from Eq. (1) we have $T=-1$, and $a_2(L)=0$. Hence, the modulation does not create any frequency conversion. Instead its sole effect is to induce an extra π phase shift in addition to the propagation phase. As a result, all power ends up as output in port 3.

We now consider the time-reversed scenario where light is injected into port 3 instead. In the modulated waveguide region, the light propagates in the backward direction, and in general the phase matching condition is not satisfied. Suppose the same modulation is strongly phase-mismatched in the backward direction, i.e.,

$$\Delta k_b\cdot L = \Delta k_b\cdot 2l_c \gg 1, \tag{4}$$

from Eq. (1) then we have $T\approx 1$. Thus, the output completely ends up in port 2. The device therefore functions as a four-port circulator that clearly exhibits strong nonreciprocal behavior.

We now discuss the physical constraints that allow Eq. (4) to be satisfied in the backward direction. For most electro-optic or acoustic-optic modulation schemes, the modulation frequency $\Omega\ll\omega_1$. In the backward direction, among all possible transitions, the one between the mode at $[\omega_1,-k_1(\omega_1)]$ and a lower frequency mode $[\omega_1-\Omega,-k_2(\omega_1-\Omega)]$ in the second band [green dot in Fig. 1(c)] has the smallest phase mismatch, as described by a $\Delta k_b=-k_2(\omega_1-\Omega)+k_1(\omega_1)-q\approx 2\Omega/v_g$. Combining with the results of coherence length [Eq. (2)], the condition of Eq. (4) is then transformed to

$$\frac{4\lambda_0}{c}\cdot\frac{\Omega}{\gamma} \gg 1. \tag{5}$$

Remarkably, we note that the effects of weak refractive index modulation and low modulation frequency cancel each other out in Eq. (5). Moreover, it is precisely such a cancellation that enables the construction of dynamic isolators with practical modulation mechanisms.

We now give a numeric example. The width of the silicon slab waveguide ($\varepsilon_s=12.25$) is chosen as $d=0.268$ μm such that the first and second bands have approximately the same group velocity for the operation wavelength around 1.55 μm. We consider a modulation frequency $\Omega/2\pi=20$ GHz and modulation strength $\delta/\varepsilon_s=5\times10^{-4}$, which can be achieved by carrier injection/extraction schemes.[11–13] The spatial period of the modulation is $2\pi/q=0.88$ μm. Such a modulation satisfies the phase-matching condition between a fundamental mode at $\omega_1/2\pi=193$ THz and a second band mode that is 20 GHz higher, both propagating in the forward direction. The resulting coherent length for this interband transition is $l_c=2.2$ mm. In the backward direction, we have $\Delta k_b l_c=6.7$, which is sufficient to satisfy the condition of Eq. (4).

We apply such modulation to one arm of the Mach–Zehnder interferometer, as shown in Fig. 1(a). The length of the modulation region is chosen to be $L=4.4$ mm. The transmission spectra [Fig. 2(a)] between ports 3 and 2 can then be obtained using the waveguide dispersion relation determined analytically, and Eq. (3). The contrast between transmissions of the opposite directions is above 20 dB for a bandwidth of 7 nm.

A dielectric constant modulation based on carrier injection also induces propagation loss. The required dielectric

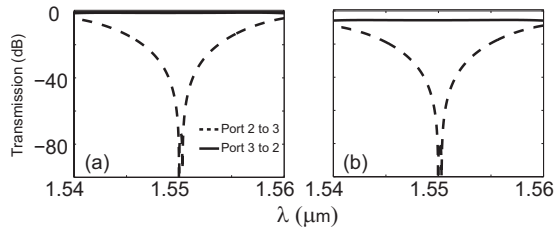

FIG. 2. The transmission spectra for the Mach–Zehnder isolator (a) without modulation loss and (b) with loss (b).

modulation strength $\delta/\varepsilon_s = 5 \times 10^{-4}$ results in a propagating loss of 1.5 cm^{-1} in silicon.[11] To balance the loss in the interferometer, the same propagation loss is applied to a region of length L in the lower waveguide. In such a situation, the insertion loss is increased to around 6.5 dB while the contrast ratio in transmission between the two counterpropagating directions remains approximately the same as the lossless case [Fig. 2(b)]. Finally, since the length of the proposed device is limited by the coherent length l_c. From Eq. (2), further miniaturization of the device is possible by either increasing the modulation strength, or with the use of slow light waveguide that reduces the group velocity.

This work is supported by the National Science Foundation (Grant No. ECS-0622212).

[1]M. Soljacic and J. D. Joannopoulos, Nature Mater. **3**, 211 (2004).
[2]R. L. Espinola, T. Izuhara, M. C. Tsai, R. M. Osgood, Jr., and H. Dötsch, Opt. Lett. **29**, 941 (2004).
[3]M. Levy, J. Opt. Soc. Am. B **22**, 254 (2005).
[4]T. R. Zaman, X. Guo, and R. J. Ram, Appl. Phys. Lett. **90**, 023514 (2007).
[5]H. Dötsch, N. Bahlmann, O. Zhuromskyy, M. Hammer, L. Wilkens, R. Gerhardt, P. Hertel, and A. F. Popkov, J. Opt. Soc. Am. B **22**, 240 (2005).
[6]M. Soljačič, C. Luo, J. D. Joannopoulos, and S. Fan, Opt. Lett. **28**, 637 (2003).
[7]K. Gallo, G. Assanto, K. R. Parameswaran, and M. M. Fejer, Appl. Phys. Lett. **79**, 314 (2001).
[8]Z. Yu and S. Fan, Nat. Photonics **3**, 91 (2009); See also S. J. B. Yoo, *ibid.* **3**, 77 (2009).
[9]J. N. Winn, S. Fan, J. D. Joannopoulos, and E. P. Ippen, Phys. Rev. B **59**, 1551 (1999).
[10]B. E. A. Saleh and M. C. Teich, *Fundamentals of Photonics*, 2nd ed. (Wiley, New York, 2007), p. 1033.
[11]R. A. Soref and B. R. Bennett, IEEE J. Quantum Electron. **23**, 123 (1987).
[12]L. Liao, A. Liu, D. Rubin, J. Basak, Y. Chetrit, H. Nguyen, R. Cohen, N. Izhaky, and M. Paniccia, Electron. Lett. **43**, 1196 (2007).
[13]Q. Xu, B. Schmidt, S. Pradhan, and M. Lipson, Nature (London) **435**, 325 (2005).